Estimation of Near-Surface Attenuation in Bedrock for Analysis of Intraplate Seismic Hazard

A.M. Chandler [1], N.T.K. Lam [2], H.H. Tsang [3], and M.N. Sheikh [3]

1. Department of Civil Engineering, The University of Hong Kong, Pokfulam Road, Hong Kong, email: amchandl@hkucc.hku.hk
2. Department of Civil and Environmental Engineering, The University of Melbourne, Parkville, Victoria 3052, Australia
3. Department of Civil Engineering, The University of Hong Kong, Pokfulam Road, Hong Kong

ABSTRACT: *The significance of near-surface attenuation in bedrock, as distinct from attenuation in unconsolidated soft soil sediments, has been identified. The k parameter, which characterizes the extent of this attenuation mechanism, is generally difficult to measure, particularly in regions of low and moderate seismicity. Empirical correlation of k with the near-surface shear wave velocity parameter in rock has been developed using global information obtained from limited independent studies. The influence of shaking intensity on the value of k has been found to be negligible in conditions that are consistent with the average seismicity of Australia (as also for other intraplate regions). Thus, adjustment in the value of k to account for variations in earthquake magnitude, or the intensity of ground shaking, has not been recommended for intraplate conditions. In parallel with the empirical correlations, values of k have also been obtained from calibration analyses employing stochastic simulations of the seismological model, along with one-dimensional non-linear shear wave analyses of the rock layers. Good agreement in the values of k obtained from the different approaches has been demonstrated. The correlation of k with the near-surface shear wave velocity of rock, as recommended in this paper, has thereby been reaffirmed.*

Keywords: Intraplate seismic hazard; Upper crust; Near-surface attenuation; Seismological model; Kappa

1. Introduction

Regional ground motion attenuation relationships for intraplate regions usually cannot be developed by conventional empirical modelling, since there is typically a scarcity of strong motion accelerogram records. Nonetheless, there are alternative means by which representative seismic hazard models for these regions can be developed. For example, in countries or regions with a long history of archival records (such as China), models can be developed from databases of iso-seismal intensity maps of historical earthquakes. However, seismic hazard information that can be inferred from historical intensity data tends to be rather generalized.

Seismological modelling has been developed to provide more specific information on the predicted ground shaking through stochastic simulations. The seismic hazard obtained from the simulation methodology may then be verified by comparison with historical intensity data. This dual approach of combining the seismological model with historical intensity data has been applied by the authors in seismic hazard modelling for South China [1] and Australia [2].

A seismological model that could be developed from a database of seismograms (such as in Central and Eastern North America, CENA) could resolve

ground shaking into its source, path and site components. Modelling for each of these components could be undertaken using a combination of a theoretical approach and empirical ground motion data. The seismological Quality Factor, Q, is amongst the many parameters required for input into the seismological model. Q defines the wave transmission quality of the earth's crust in the study region. The Spectral Ratio Method and the Coda Wave Method, that are based on observing the decay of low intensity ground motion with distance (or time) [3], are amongst the methods that have been devised to conveniently measure the regional Q factor. Q-factors for different regions within China have also been inferred from historical intensity data [4]. Using one of these techniques, the Q parameter has been modelled in several regions of low and moderate seismicity, in which strong motion data is lacking.

The value of Q obtained from seismological monitoring can be substituted into Eq. (1) to develop the filter function $An(f)$ which represents the effects of whole path attenuation of seismic waves propagating within the earth's crust:

$$An(f) = e^{-\frac{\pi . f . R}{Q V_S}} \tag{1}$$

where f is the wave frequency, R is the length of the wave travel path and V_s is the shear wave velocity.

The filter function defined by Eq. (1) may be combined with other filter functions representing various source, path and site effects to predict the Fourier spectrum of seismic waves reaching the ground surface. The developed spectral information may then be used for generating artificial ground motions using stochastic simulations (as reviewed in Ref. [5]). The simulated accelerograms may then be subject to response spectrum analysis for engineering applications.

It has been found from such simulation studies [6] that regional variations in the Q factor will only have engineering significance for distant earthquakes with epicentral distances exceeding around 70*km*.

In fact, the regional Q factor as measured by any one of the methods described above only represents a part of the total attenuation experienced by seismic waves on reaching the ground surface. A considerable amount of attenuation is experienced during transmission through the upper layers of the earth's crust, including unconsolidated soft soil sediments. This attenuation mechanism is always accompanied by associated amplification mechanisms. Unless drill-holes have been suitably instrumented, neither of the above mechanisms can be studied by observing the decay, or amplification, of the seismic wave with distance, since the change in wave amplitudes occurs over very short distances within the wave transmission path. The combined attenuation-amplification effects are often treated as site effects (or soil modification effects) that could be modelled by one-dimensional shear wave analysis (for example, using the well-known computer program SHAKE [7]).

It is noted that site response analyses undertaken by engineers usually only consider the wave modification properties of soil sediments overlying bedrock, and not those modifications that occur within the bedrock itself, despite the latter's significance. Importantly, wave transmission quality within bedrock is not uniform with depth. Near-surface attenuation (also known as "upper-crust" attenuation) occurs over a very short transmission distance, as for attenuation in soft soil sediments. Ref. [8] identified that 90% of the total attenuation of seismic waves in Californian bedrock occurred within the upper 4*km* of the earth's crust. As previously mentioned, attenuation of this nature, though significant, cannot be captured by methods which are based on monitoring the decay of wave intensity with distance (for example, the Spectral Ratio Method referred to above).

A range of methods has been used to measure the near-surface attenuation properties in bedrock. However, near-surface attenuation still remains an element of uncertainty in most parts of the world, due to difficulties with its measurement as well as ambiguities in the definition of the associated attenuation parameter (see Section 3.2 for further details). When this important mechanism has not been ascertained, a reliable seismological model for the region is difficult to develop.

This paper is aimed at contributing to the development of a robust methodology by which the extent of near-surface attenuation can be estimated.

The filter function, $P(f)$, that can be used to represent near-surface attenuation in the seismological model has been defined by Eq. (2):

$$P(f) = e^{-\pi f \kappa} \tag{2}$$

where the parameter κ (in units of seconds and pronounced "Kappa") is used to represent the combined factor R/QV_s in Eq. (1). Each of the variables in this factor has been assigned the subscript

"*uc*", which denotes contributions by the upper crust. Thus:

$$\kappa = R_{uc} / (Q_{uc} V_{uc}) \quad (3)$$

Given that around 90% of the crustal attenuation, defined herein as near-surface attenuation, has been found to occur in the upper 4*km* of the earth's crust, the value of R_{uc} has been taken as a constant equal to 4*km*. The value of Q_{uc} represents the Q value within the upper crust and is the parameter this study aims to model. Finally, V_{uc} is the average shear wave velocity of the upper crust, defined by Eq. (4):

$$V_{uc} = \frac{R_{uc}}{\sum_i \frac{d z_i}{V_{s_i}}} \quad \text{or} \quad \frac{R_{uc}}{\int_0^{R_{uc}} \frac{d z}{V_s}} \quad (4)$$

where i is layer number, each having finite depth dz_i.

This paper first explores the correlations between the κ (and the Q_{uc}) parameters, along with the associated parameters described above, with the shear wave velocity of the bedrock near to the ground surface (Section 2). The latter velocity parameter has been selected, as it is straightforward to measure in the field. The variation of the extent of near-surface attenuation with the intensity of the ground shaking has further been investigated in Section 3. Analytical modelling using wave analysis was then undertaken to model near-surface attenuation. Results obtained by this different approach have been presented in Section 4, and provide support for the empirical correlations developed in Sections 2 and 3.

2. Measurement and Modelling for the κ Parameter

2.1. Measurements of the κ Parameter

As mentioned in Section 1, near-surface attenuation properties of the earth's crust cannot be inferred from the rate of attenuation of ground motion amplitude with increasing epicentral distance. Thus, near-surface effects have not been distinguished from source effects in conventional attenuation models. However, the measurement methods described in this section enable near-surface attenuation and the associated κ parameter to be measured.

In the method developed in Ref. [9], the Fourier transform of the recorded accelerations is first taken and plotted versus frequency with a log-linear scale. Accelerograms used in conjunction with this method were typically recorded from events of magnitude M4-M7. The value of κ may then be inferred from the slope of the straight-line fitted between the corner frequency (less than 5*Hz* for $M >$ 4) and the upper frequency limit (typically at 15-30*Hz*) of the spectrum. Using this method, a κ value equal to 0.04 has been identified for California [9], κ = 0.07 for the southern and central Apennines in Italy [10] and κ = 0.011 in British Columbia [11]. The measured κ parameter could have represented also some whole path attenuation in the deeper (higher quality) rock crust, depending on the epicentral distance from which measurements were taken. Such contributions from whole path attenuation could be resolved by plotting the apparent values of κ with epicentral distance. The "*true*" value of κ representing purely near-surface attenuation, denoted in the literature as κ_o could then be obtained [9] by extrapolating the linear trend of versus epicentral distance to "*zero*" epicentral distance. In this paper, both parameters κ and κ_o which may be used interchangeably, represent solely the near-surface attenuation.

The measured κ parameter could also have included the significant effects of upper-crustal amplification, which co-exists with the upper-crustal (near-surface) attenuation. In attempts to eliminate these amplification components in the measurement of κ, a seismological model that has resolved near-surface effects into numerous attenuation and amplification components was first developed [12]. Fourier spectra simulated from the seismological model assuming a range of trial values of κ were then compared with the spectrum determined from the recorded ground motion, in order to identify the "best matched" spectra. This method of matching spectra, which is distinguished from the method in Ref. [9], provides non-unique estimates of κ. This is because the estimated κ value would depend on the frequency functions that have been incorporated into the seismological model. This method of measurement which was adopted in Ref's [12] and [13], predicts higher κ than those determined by the original method introduced in Ref. [9]. However, the discrepancy is generally rather small (only 0.006sec for California).

There also exists significant trading-off between κ and the assumed stress-drop level. Stress-drop varying between 30 bars and 600 bars has been assumed in Ref's [13-16], for different regions within Italy and Europe. Considerable uncertainties in the actual value have been associated with such estimates, because of the stress-drop variability.

In the study for Switzerland [17], $\kappa = 0.015$ was recommended based on the very low stress-drop level of 5-10 bars. A significantly higher κ value would have been estimated had the modelled stress drop level been increased. In Ref. [18], $\kappa = 0.04$ was recommended for Central Mexico, but details of the measurements have not been reported. Neither of these studies has been included in the listing given herein in Table (1).

Estimates of κ have also been proposed for other parts of the world in studies including Ref's [19-22], but the recommendations were based only on measurements reported elsewhere. These references have similarly not been included in Table (1). Ref's [23-24] have also not been enlisted (due to insufficient information to complete all column entries in the table).

The κ parameter could alternatively be determined by observing the decay of the Coda wave envelope with time [25], but the observations must be made at shallow depths and very close to the epicentre of the earthquake in order that only a small volume of the earth's crust close to the surface (within the upper 3 to 4*km*) is included in the measurement. The value of or the Quality factor of the upper crust, Q_{uc}, could be calculated from the ratio of the envelope amplitude observed for a range of specified frequencies. Recordings close to the earthquake epicentre are scarce in low and moderate seismic regions, but earthquake swarms offer excellent opportunities for this type of measurement.

2.2. Correlation of Q_o and the k Parameter with Shear Wave Velocity

It is evident from the above review and discussion that it is generally difficult to measure κ in regions of low and moderate seismicity, where recordings from local moderate and large magnitude earthquakes in the near field are either non-existent or, at best, scarce. It is proposed that the value of κ be estimated in accordance with its correlation with parameters that can be identified most easily from normal engineering investigations; for example, near-surface shear wave velocity that can be inferred from shallow drill-hole records and hence is generally available. The objective of this section is to develop such correlations.

First, published values were collated for the regional seismological Quality factor Q ($=Q_o$ at frequency of 1*Hz*). The Quality factor Q, compared with κ, is a more commonly known parameter in different regions around the world. The databases that have been sourced include Ref's [3, 4, 5, 10, 13, 14, 22, 26]. For each region from which the Q value was reported (as listed in Table (2)), the corresponding value of S-wave velocity at the shallow reference depth of 0.03*km* (30*m*), termed $V_{s,\,0.03}$, was identified using the global crustal model CRUST2.0 [27], developed originally in Ref. [28]. The correlation between Q_o and $V_{s,\,0.03}$ so obtained from the survey has been shown in Figure (1).

It is noted that the value of Q obtained from seismological monitoring depends on the modelling assumptions adopted in each individual study. For example, there is some trading-off between geometrical and anelastic attenuation (with the latter represented by the Q-factor). Thus, different assumptions with regard to the geometrical attenuation would result in different anelastic attenuation, and hence Q-factor. Furthermore, the epicentral distances and direction of the wave transmission path in the monitored earthquakes would also affect the Q values being reported. It is noted that Q has been obtained from a multiplicity of studies employing different methodologies. Consequently, there exists considerable scatter in the correlations presented in Figure (1). Even with these measurement uncertainties, the close link between regional transmission quality of the rock and the shear wave velocity (i.e. Q_o versus $V_{s,0.03}$) is evident.

Table 1. Published values of κ and Q_o, and the implied values of Q_{uc} and Q_{uc}/Q_o ratio.

	Published k	Published Q_o	Assumed R_{uc} (km)	Assumed V_{uc} (km/s)	Implied Q_{uc}	Implied Q_{uc}/Q_o
Central and Southern Apennines, Italy [13]	0.070	100	4	2.3	25	0.25
Northeastern Italy [16]	0.045	260	4	2.3	39	0.15
Central Europe [18]	0.05	400	4	2.3	35	0.09
Umbria-Marche Apennines, Italy [17]	0.04	130	4	2.3	43	0.33
British Columbia [14]	0.011	380	4	3.0	121	0.32
Generic Rock [15]	0.035-0.04	204	4	2.4	42-48	0.20-0.23
California [12]	0.040	204	4	2.4	42	0.20

Table 2. Databases of Q_0 and κ values shown in Figures (1) and (2).

	Assumed $V_{s,0.03}$(km/s)	Published Q_0	Ref.	Published k (s)	Ref.
Central and Eastern	2.8	1000	5	0.003	*
North America	2.8	900	5	0.003	*
	2.8	755	5	0.004	*
	2.8	670	5	0.004	*
	2.8	500	5	0.006	*
Western North America	0.7	150	5	0.066	*
	0.65	150	5	0.073	*
	0.7	110	5	0.069	*
Sino-Korean	1.2	342	5	0.022	*
Paraplatform	1.2	189	5	0.039	*
	1.2	293	5	0.025	*
	1.2	400	5	0.019	*
South China Fold	1.5	482	5	0.014	*
System	1.5	370	5	0.018	*
	1.5	256	5	0.027	*
	1.5	240	5	0.028	*
Australia	2.4	500	5	0.012	*
	0.65	50	5	0.045	*
	0.65	200	5	0.040	*
	2.35	550	5	0.011	*
Southern Iberia	0.48	150	5	0.069	*
NE Japan	0.53	47	5	0.067	*
Taiwan	0.48	149	6	0.081	*
Generic Hard Rock	2.8	680	7	0	7
Generic Rock	0.85	204	7	0.040	7
Apennines, Italy	0.62	100	13	0.070	13
Northeastern Italy	0.62	260	16	0.045	16
Apennines, Italy	0.62	130	17	-	-
Southern California	0.7	180	23	0.056	*
Iceland	0.65	-	-	0.040	19
Generic Rock	0.85	204	15	0.035	15
NEHRP Site Class C	0.7	-	-	0.048	20
	1.0	-	-	0.04	20
	0.74	-	-	0.05	22
Eastern North America	2.8	-	-	0.006	21

* The corresponding κ value has been inferred using the methodology described in Ref. [11].

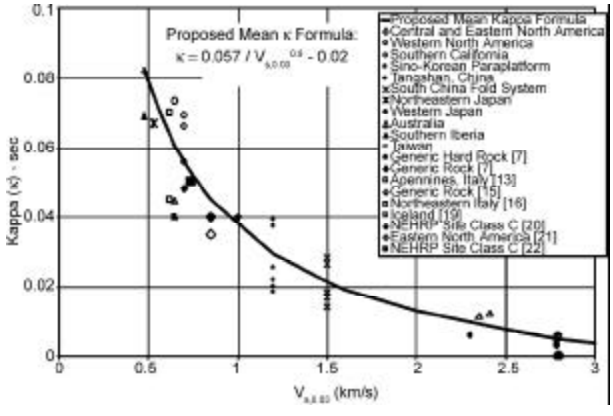

Figure 1. Relationship between the upper-crust attenuation parameter κ and $V_{s,0.03}$, derived from global data.

The value of $V_{s,0.03}$ is also subject to considerable uncertainty. The value as inferred from the global crustal model [27] can be checked by comparison with local measurements. However, note that $V_{s,0.03}$ is subject to significant variations between different sites within the same region. Thus, a representative sample of local measurements will have to be collected and averaged in order that a regional measured value can be obtained.

Correlation between the two arrays: average Q_o versus $V_{s,0.03}$ has been presented in Figure (1) and represented mathematically by Eq. (5):

$$Q_o = 60 + 319(V_{s,0.03} - 0.48)^{0.8} \qquad (5)$$

$$[0.5km/s \leq V_{s,0.03} \leq 3.0km/s]$$

Second, the correlation adopted for modelling Q_o has been extended to the modelling of Q_{uc} and κ. The purpose is to enable the upper-crust attenuation property to be linked directly to a commonly determined engineering parameter, namely $V_{s,0.03}$.

Incorporated into Table (1) are the recommendations by a number of seismological investigations reviewed in Section 2.1. For each of the studies listed in Table (1), the value of Q_{uc} was calculated using Eq. (3), based on the tabulated value of κ (see Column 2). Further, V_{uc} was determined from Eq. (4) (with the S-wave velocity profile defined by the functional form developed in Ref. [29] along with the parameters provided by the CRUST2.0 model [27]) and a constant value of R_{uc} (= $4km$) was assumed. Also given in Table (1) is the Q_o value, which has been determined for the same region. The ratio of Q_{uc}/Q_o inferred from the different studies is shown to have a median value of about 0.2. However, as a result of different modelling assumptions there exists considerable scatter in the individual estimates that vary from this median value by up to some 50%. Thus, developing a rigorous model for defining the ratio for Q_{uc}/Q_o is not considered justified. Instead, a constant ratio of Q_{uc}/Q_o = 0.2 has been assumed herein.

It was found from seismological studies in southeastern Australia based on the measurement of Coda wave envelopes that the value of Q_{uc} is some 20% of the value of Q_o [25], which is consistent with the trend revealed in Table (1).

The median Q_{uc}/Q_o ratio of 0.2 was then applied to each of the regions from which the data in Figure (1) was plotted. In each case, the value of Q_{uc}, V_{uc} and R_{uc} (= $4km$) was identified for substitution into Eq. (3), in order that the value of κ could

be evaluated along with the value of Q_o that was known originally. A new array of κ values (as listed in Table (2)) was then created for correlation with the $V_{s,0.03}$ array, as shown in Figure (2) and represented mathematically by Eq. (6):

$$\kappa = \left(\frac{0.057}{V_{s,0.03}^{0.8}} - 0.02 \right) [0.5 km/s \le V_{s,0.03} \le 3.0 km/s] \quad (6)$$

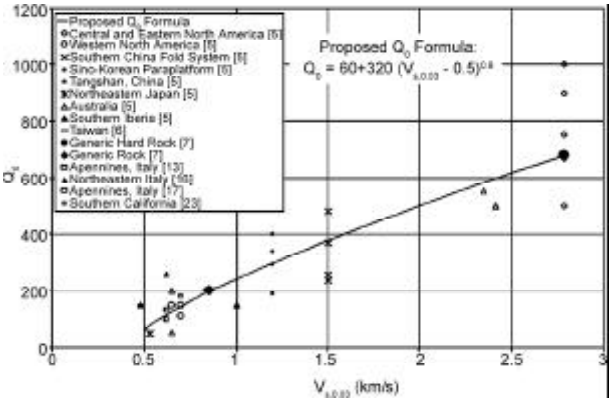

Figure 2. Relationship between Q_0 and $V_{s,0.03}$ from global data.

Eq. (6) based on Figure (2) is the key outcome of this stage of the study and can be further supported by numerous studies, Ref's [5, 10, 12, 13, 20, 22, 30, 31]. The observed scatter ultimately is due to the fact that the crustal shear wave velocity profile can vary significantly, even with a uniform value of $V_{s,0.03}$. Furthermore, influence by parameters that affect crustal damping properties could also contribute to the scatter. It is evident that the scatter would be much smaller with a model that has incorporated a larger number of such parameters. However, if the model is to be of practical engineering value, information on the parameters must be readily available before being included in the modelling. At the present time, $V_{s,0.03}$ is much more straightforward to obtain than other parameters, in the context of normal engineering practice.

Finally, with regard to the velocity parameter $V_{s,0.03}$, if consideration is given to the shear wave velocity relationship established in Ref. [29] for the Upper Sedimentary Layer, it may be shown that the shear wave velocity averaged over the upper 0.03*km* (30*m*) rock layers is in the order of 0.75 $V_{s,0.03}$. As it is common practice in existing seismic codes of practice to use such average velocity to define the soil or rock class, a useful alternative formulation is to replace $V_{s,0.03}$ in Eq. (6) by 1.33 times the velocity averaged over the upper 30*m* depth in rock.

3. Dependence of k on Magnitude and Intensity

As is widely known, hysteretic damping in both structures and soil is dependent on the amplitude of the material deformation. Thus, the κ parameter should increase with increasing deformation of the rock crust, which in turn is controlled by the intensity of shaking in the bedrock. Seismological studies [32-33] developed expressions defining the effects the earthquake magnitude have upon κ (which is based on the fact that the intensity of ground shaking increases with increasing magnitude, for any given epicentral distance).

Guided by recommendations from the two studies, a formula relating κ to the earthquake magnitude *M* (for *M*5 to *M*7.5), has been proposed herein [Eq. (7)], for Generic Rock (*GR*) conditions of Western North America (*WNA*), in which $V_{s,0.03}$ = 0.85*km/s*, see also to Figure (3).

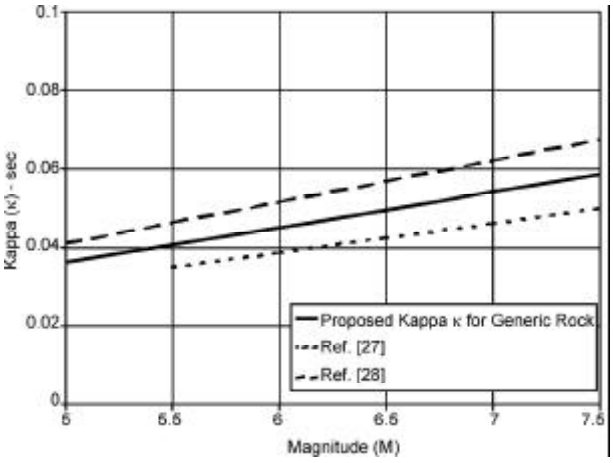

Figure 3. Variation of κ predictions for Western North America with earthquake magnitude M.

$$\kappa = 0.045 \left(1 + \frac{M-6}{5} \right) [V_{s,0.03} = 0.85 km/s, WNA] \quad (7)$$

Eq. (7) uses *M*6 earthquakes as the reference earthquake scenario, and the corresponding reference κ value has been taken as 0.045. It is indicated in the expression that the percentage change in the value of κ for a change in *M* of 0.5 (±) is in the order of 10%.

It is noted that the mean correlation developed in Section 2, see Figure (2) and Eq. (6), has the value of κ equal to 0.045 at $V_{s,0.03}$ = 0.85*km/s*. Thus, Eqs. (6) and (7) are compatible, which also means that Eq. (6) is consistent with the reference *M*6 earthquake scenario.

The empirical expressions of Eqs. (6) and (7) have accordingly been combined herein to provide a generalized magnitude (M)-dependent prediction formula for κ, as in Eq. (8):

$$\kappa = \left(\frac{0.057}{V_{s,0.03}^{0.8}} - 0.02 \right) \left(1 + \frac{M-6}{5} \right) \qquad (8)$$

$[0.5km/s \leq V_{s,0.03} \leq 3.0km/s]$

Results obtained using Eq. (8) have been presented in Figure (4) for the considered range of $V_{s,0.03}$ and for $M5.5$, $M6.5$ and $M7.5$ (along with the reference mean curve for $M6$).

The M-dependent relationships defined by Eqs. (7) and (8) have been based upon the recommendations (for *WNA*) in Ref's [32-33], in which ground motion data collected from *WNA* was analysed.

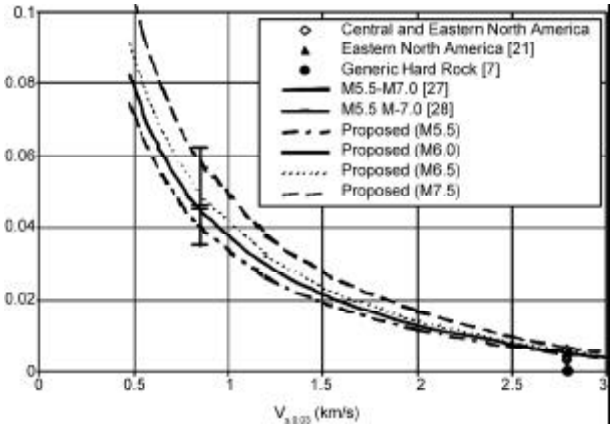

Figure 4. Variation of κ with $V_{s,0.03}$ for M5.5, M6.5 and M7.5, and also the mean curve of κ (for M6). Results for proposed relationship have been obtained using Eq. (6).

Based on the intuition that κ should increase with the level of ground shaking, then clearly relating κ only to M, and not also to the source-site distance R, seems to imply that the earthquake database used in these studies could be mostly near-field events. The generality of the developed expression is therefore questionable. In investigating this issue further, the authors referred to the M-R combinations of the earthquake database presented in Figure (3) on page 261 of Ref. [34]. The M-R combinations were sorted such that only events with $M5$ and R = 10-40km were considered, and this actually included a high proportion of records originally incorporated in the database.

With each such M-R combination, the value of κ was calculated using Eq. (8), along with the intensity of ground shaking. The Spectral Intensity (SI) parameter introduced in Ref. [35] was used as the parameter in quantifying the intensity. SI (with units of metres) is defined as the area under the velocity response spectrum between periods T = 0.1sec to T = 2.5sec. In determining SI, synthetic accelerograms were simulated for each M-R combination using computer program *GENQKE* [36] and the crustal model for Generic Rock of *WNA* [12]. The correlation of κ with the intensity parameter SI was then obtained, as shown in Figure (5). It is noted that the presented correlation is only an approximation to the actual correlation, since the value of κ calculated for each event was based on Eq. (8) and not on original measurements. Moreover, the calculated intensity was based on simulated motions and not from the original recorded motions. Despite these approximations, Figure (5) suffices to delineate the basic trend.

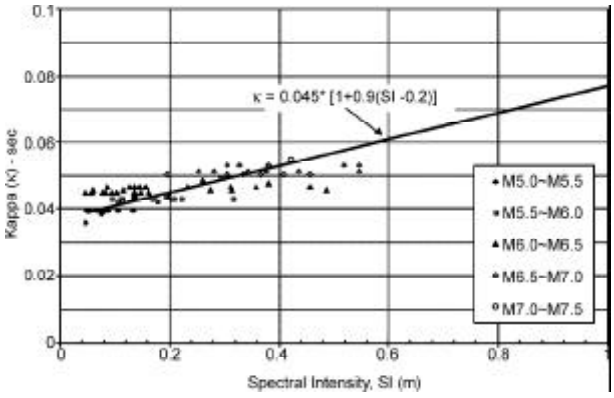

Figure 5. Relating κ to Spectral Intensity based on Western North America earthquake database [27, 29] for $M \geq 5$ and R in the range 10-40km.

Figure (5) indicates that the reference value of $\kappa = 0.045\sigma$ corresponds to SI= 0.2m. The dependence of κ on the earthquake intensity parameter, SI, has accordingly been defined by the following expression:

$$\kappa = 0.045\left[1 + 0.9\left(SI - 0.2\right)\right] \; SI \text{ in } m \qquad (9)$$

where 0.2m is the reference value of SI.

The second bracketed term in Eq. (8), that defines the dependence of κ on the earthquake magnitude, can now be replaced by the square bracketed term shown in Eq. (9), which is taken to be generic (meaning that it can be applied to any seismic region and not just to *WNA*).

Individual M-R combinations that were involved in the analysis and the corresponding values of SI have been plotted in Figure (6). SI=0.1m has been shown to be associated with earthquake scenarios of

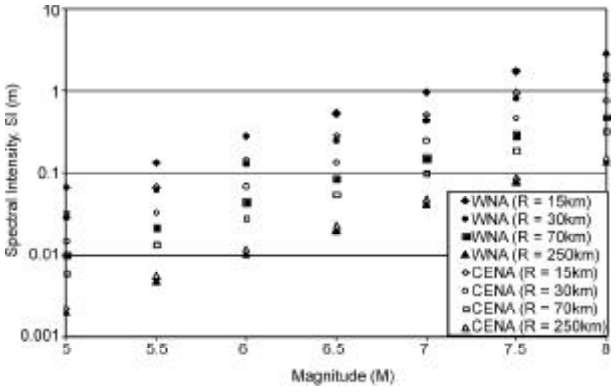

Figure 6. Relating Spectral Intensity to magnitude based on Western North America (WNA) and Central and Eastern North America (CENA) M-R combinations.

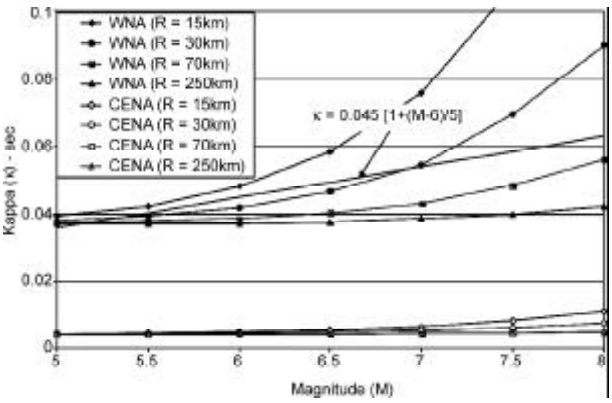

Figure 7. Relating κ to magnitude (M) based on Western North America (WNA) and Central and Eastern North America (CENA) M-R combinations.

*M*5.5 at *R*=15*km*, *M*6 at *R* = 30*km* or *M*7 at *R*=70*km*. The first of these three scenarios is similar to the well-publicised 1989 Newcastle earthquake, New South Wales, Australia (except that the epicentral distance was around 11-12*km* instead of 15*km*). The *MMI* recorded on rock sites was *VII*, implying a peak ground velocity, *PGV*, in the order of 90*mm/sec* [37]. The *PGV* is accordingly about 60*mm/sec* if the epicentral distance has been corrected to 15*km*. The second scenario is estimated to have a *PGV* also in the order of 60*mm/sec* [2]. The 500-year return period seismic loading stipulated in the current earthquake loading standard [38] for the majority of Australian capital cities was based on this *PGV* level of 60*mm/sec*, which corresponds to an acceleration coefficient of 0.08*g*. If a typical "1.8" multiplier is used to extend the predictions from a return period of 500 years to 2500 years, the value of *SI* is increased from about 0.1*m* to 0.2*m*. It is shown in Figure (5) that the value of κ varies by only 0.005*s* (from 0.04*s* to 0.045*s*) over this range of *SI*, which is representative of average intraplate seismicity. Applying adjustment of this magnitude to the value of κ therefore does not seem to be justified, given the uncertainties in the prediction.

The information presented in Figures (5) and (6) has been combined and presented in Figure (7), which shows κ to remain effectively constant at around 0.04*s* for the three earthquake scenarios considered above. Clearly, the intensity effects on the value of κ have been overstated by the magnitude-dependent factor of Eq. (6), also annotated in Figure (7).

In summary, it is recommended that no adjustment for the effects of magnitude, nor intensity, is required for the relationship developed in Section 2, see Figure (2) and Eq. (6), provided the *PGV* on rock sites is below 110*mm/sec* (i.e. 1.8x 60*mm/sec*), or if *SI* is smaller than 0.2*m*.

4. Determination of k Parameter by Calibration

4.1. One-Dimensional Shear Wave Analysis

It should be noted that the correlation of κ with the rock shear-wave (S-wave) velocity, as developed in Sections 2 and 3, was based on limited measurements taken from the field. Furthermore, it is acknowledged that the energy absorption properties of the earth's crust have not been fully reflected in its shear wave velocity. Notwithstanding the above, it is considered important to develop the correlation for practical applications, when only shear wave velocity information is available. What is desirable is support for the correlations by an independent analytical modelling approach, as opposed to the empirical modelling approach.

As stated in Section 1, the energy absorption behaviour of unconsolidated soft soil sediments may be modelled by one-dimensional (1-D) non-linear shear wave analysis using computer programs such as SHAKE [7]. It is considered viable to adapt such analysis for modelling κ, although normally this type of analysis would seldom incorporate the attenuation behaviour of the bedrock. This section explores the use of this analytical approach to provide independent support for the empirical correlations developed in Sections 2 and 3.

Rock layers 5*km* deep have been modelled for 1-*D* non-linear shear wave analysis using the well-known SHAKE program [7]. These rock layers were then subject to simulated excitations applied at the 5*km* deep base. The time histories of the applied

excitations were simulated using computer program GENQKE [36]. The simulations were based on conditions very close to the source of the earthquake.

In SHAKE analysis, the equivalent linear method is used normally to account for non-linearity in the soil layers using an iterative procedure. In this study, similar analyses have been applied to the rock layers. Initially, a set of properties (shear modulus, damping, and total unit weight) has been assigned to each soil (or rock) sub-layer. Using these properties, the shear strain induced in each sub-layer has been calculated. The shear modulus and the damping ratios for each sub-layer have then been modified based on the applicable relationships relating these two properties to shear strain. The analysis has been repeated until strain-compatible modulus and damping have been achieved.

4.2. Stiffness Degradation and Damping Parameters for Rock

Stiffness degradation (G/G_o) ratio, or the associated damping ratio, expressed as a function of the shear strain have been well publicised in the literature for sand and clay, but similar information relating to rock has been scarcely reported. Ref. [7], however, proposed some damping and degradation curves for "average rock". Although a clear definition for this rock type has not been given in the cited publication, a shear wave velocity of some 1500*m/sec* (5000*ft/sec*) was shown at the surface of the bedrock in the worked examples.

In a recent publication [39], a generic empirical relationship for stiffness degradation in mudstone, characterised by two constants *B* and *n*, was proposed. The constant *B* represents the threshold shear strain, above which the G/G_o degradation curve falls below unity, indicating the initiation of degradation of the rock material. The constant *n* is used to determine the shape of the degradation curve, with a higher value of *n* representing a higher rate of degradation of the rock material. The degradation curve of Ref. [7] has been shown to match very closely with that proposed in Ref. [39] if *B* and *n* are taken equal to 50,000 and 0.8, respectively, see Figure (8). Strictly speaking, different rock types possess different values of *B* and *n*. However, the precision of the modelling for degradation does not seem to be critical in regions of low and moderate seismicity, in view of the generally low demand on the shear strains. Consequently, the same values of *B* and *n* have been assumed below, for the analyses of the different rock types.

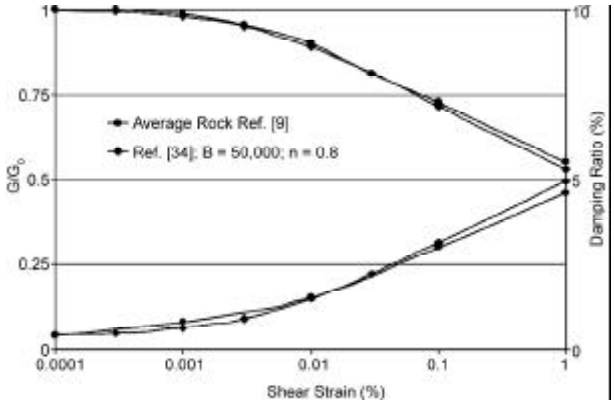

Figure 8. Degradation and damping curves for average rock.

Material damping is actually closely related to the degradation of the dynamic shear modulus, since both mechanisms depend directly on the cyclic stress-strain behaviour of the crustal materials, as explained in Ref. [40]. The damping model to be presented in the following has been based on this important link.

Ref. [41] conducted cyclic tri-axial tests on a wide range of sedimentary soft rock (having shear wave velocity ranging between 300*m/s* and 2500*m/s*), and recommended that the damping ratio be estimated by the generic expression of Eq. (10):

$$D = D_{max}(1 - G/G_o) + D_{min}(G/G_o) \qquad (10)$$

where D = damping ratio (%)

D_{max} = Maximum damping ratio (characterizing fully degraded conditions)

D_{min} = Minimum (initial) damping ratio characterizing low strain conditions

The damping ratio (%) for a given rock class can be obtained by substituting the degradation ratios [39], along with the corresponding D_{max} and D_{min} parameters, into Eq. (10). It has been shown in Figure (8) that the damping ratio estimated in Ref. [39] [in conjunction with Eq. (10)] and in Ref. [7] for average rock matches if D_{max} and D_{min} have been taken as 10% and 0.4%, respectively.

Further, Ref. [42] conducted resonant column tests on a wide range of residual soils (including Saprolites) and proposed that the degradation ratio be defined in accordance with Eq. (11):

$$G/G_o = 1/[1 + a*(\gamma)^b]^c \qquad (11)$$

where γ = shear strain amplitude in percent; *a*, *b*, and *c* are regression coefficients. The values of *a*, *b*, and *c* for Saprolites at a confining pressure of 100*kPa* are 617, 1.12 and 0.25, respectively. Initial damping

(D_{min}) has also been reported at around 3% in the study.

Highly accurate modelling for D_{max} in different rock classes is not warranted in an intraplate environment, in view of the low level of shear strains that is expected within the bedrock. A uniform value of D_{max} = 10% consistent with results reported in Ref. [7] has therefore been adopted herein.Importantly, the response behaviour of the bedrock is considered to be much more sensitive to initial viscous damping, which is controlled by the D_{min} parameter.

General information on damping in rock has been reported by a number of researchers [41-44]. Damping ratio would generally increase with strain and vary with the confinement pressure. At low strain level (ranging 10^{-5}-10^{-6}), the reported values of damping ratio are in the range of 0.1%-4%. At high strain level, the damping ratio can vary between 2% to 17%, the higher values corresponding to low levels of confining pressure (indicated by a shear wave velocity less than 400*m/s*).

More definitive published information on the degradation and damping properties for different rock classes are, however, not available. Thus, simple assumptions have been made herein. For example, damping properties estimated for average rock (D_{min} = 0.4% at $V_{s,30}$=1500*m/s*) and residual soils (D_{min} = 3% for $V_{s,30}$ =200-300*m/s*) provide the constraints for the modelling of D_{min} for the different rock classes, see Figure (9).

Three rock classes namely "soft", "average" and "hard" are defined herein. The soft rock layers were modelled in accordance with the Generic Rock profile [12], in which the shear wave velocity at a depth of 30*m* (i.e. $V_{s,30}$) is in the order of 600-800*m/s*. The average rock layers were modelled in accordance with a Granitic rock profile, with $V_{s,30}$ equal to 1500*m/s*. Finally, the hard rock layers were modelled with $V_{s,30}$ equal to 2500*m/s*. See Figure (10) for the shear wave velocity profile for each defined rock class.

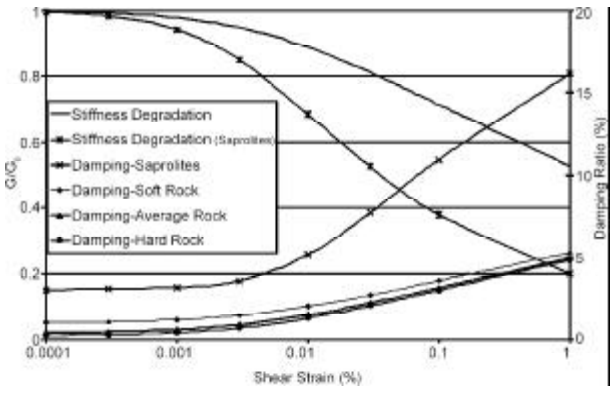

Figure 9. Degradation and damping curves for soft, average and hard rock layers in comparison with residual soil (Saprolites).

Based on the identified constraints, the value of D_{min} has been taken to reduce linearly with increase of the respective rock shear wave velocity at a representative depth of about 1*km* (given that energy absorption is expected to occur mainly in the upper 2km of the earth's crust in view of the S-wave velocity profiles of Figure (10)). As shown in Figure (10), the "representative" S-wave velocity for soft, average and hard rock is approximately 2500, 3000 and 3200 m/sec, respectively. If D_{min} is fixed (as above) at 3% for Saprolitic materials (for which the "representative" S-wave velocity may be taken as 300*m/s*) and 0.4% for average rock, by linear interpolation the damping parameter D_{min} is accordingly in the order of 1.0% and 0.2% for soft and hard rock, respectively.

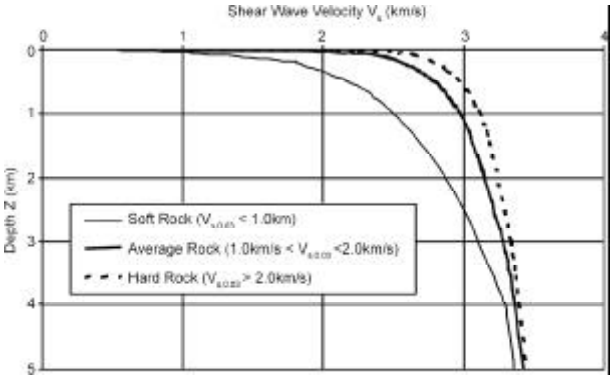

Figure 10. Shear wave velocity profiles of soft, average and hard rock layers.

The damping and shear wave velocity parameters assumed for the various rock classes may be summarised as follows:

(i) D_{max} = 10% and D_{min} = 1.0% for soft rock ($V_{s,30}$ <1000m/s);

(ii) D_{max} = 10% and D_{min} = 0.4% for average rock (1000*m/s*<$V_{s,30}$<2000*m/s*);

(iii) D_{max} = 10% and D_{min} = 0.2% for hard rock ($V_{s,30}$ >2000*m/s*).

The degradation and damping curves modelled for the different rock classes have been shown along with that determined for residual soil (Saprolites) in Figure (9).

(D_{min}) has also been reported at around 3% in the study.

Highly accurate modelling for D_{max} in different rock classes is not warranted in an intraplate environment, in view of the low level of shear strains that is expected within the bedrock. A uniform value of D_{max} = 10% consistent with results reported in Ref. [7] has therefore been adopted herein.Importantly, the response behaviour of the bedrock is considered to be much more sensitive to initial viscous damping, which is controlled by the D_{min} parameter.

General information on damping in rock has been reported by a number of researchers [41-44]. Damping ratio would generally increase with strain and vary with the confinement pressure. At low strain level (ranging 10^{-5}-10^{-6}), the reported values of damping ratio are in the range of 0.1%-4%. At high strain level, the damping ratio can vary between 2% to 17%, the higher values corresponding to low levels of confining pressure (indicated by a shear wave velocity less than 400*m/s*).

More definitive published information on the degradation and damping properties for different rock classes are, however, not available. Thus, simple assumptions have been made herein. For example, damping properties estimated for average rock (D_{min} = 0.4% at $V_{s,30}$=1500*m/s*) and residual soils (D_{min} = 3% for $V_{s,30}$ =200-300*m/s*) provide the constraints for the modelling of D_{min} for the different rock classes, see Figure (9).

Three rock classes namely "soft", "average" and "hard" are defined herein. The soft rock layers were modelled in accordance with the Generic Rock profile [12], in which the shear wave velocity at a depth of 30*m* (i.e. $V_{s,30}$) is in the order of 600-800*m/s*. The average rock layers were modelled in accordance with a Granitic rock profile, with $V_{s,30}$ equal to 1500*m/s*. Finally, the hard rock layers were modelled with $V_{s,30}$ equal to 2500*m/s*. See Figure (10) for the shear wave velocity profile for each defined rock class.

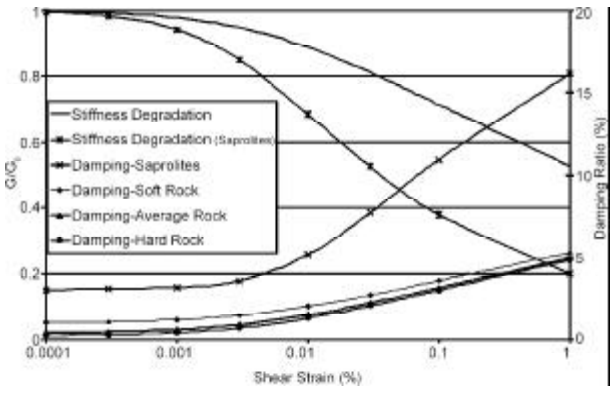

Figure 9. Degradation and damping curves for soft, average and hard rock layers in comparison with residual soil (Saprolites).

Based on the identified constraints, the value of D_{min} has been taken to reduce linearly with increase of the respective rock shear wave velocity at a representative depth of about 1*km* (given that energy absorption is expected to occur mainly in the upper 2km of the earth's crust in view of the S-wave velocity profiles of Figure (10)). As shown in Figure (10), the "representative" S-wave velocity for soft, average and hard rock is approximately 2500, 3000 and 3200 m/sec, respectively. If D_{min} is fixed (as above) at 3% for Saprolitic materials (for which the "representative" S-wave velocity may be taken as 300*m/s*) and 0.4% for average rock, by linear interpolation the damping parameter D_{min} is accordingly in the order of 1.0% and 0.2% for soft and hard rock, respectively.

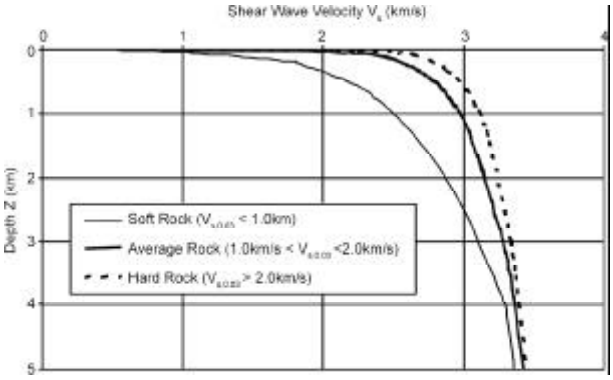

Figure 10. Shear wave velocity profiles of soft, average and hard rock layers.

The damping and shear wave velocity parameters assumed for the various rock classes may be summarised as follows:

(i) D_{max} = 10% and D_{min} = 1.0% for soft rock ($V_{s,30}$ <1000m/s);

(ii) D_{max} = 10% and D_{min} = 0.4% for average rock (1000*m/s*<$V_{s,30}$<2000*m/s*);

(iii) D_{max} = 10% and D_{min} = 0.2% for hard rock ($V_{s,30}$ >2000*m/s*).

The degradation and damping curves modelled for the different rock classes have been shown along with that determined for residual soil (Saprolites) in Figure (9).

5. Conclusions

(a) The significance of near-surface attenuation in bedrock has been identified.

(b) The κ parameter, which characterizes the extent of near-surface attenuation, is generally difficult to measure in regions of low and moderate seismicity because of magnitude or epicentral distance requirements associated with the measurements. The value of the parameter is non-unique and is dependent on the trading-off of the attenuation factor with other factors in the seismological model. The observed variability in the κ value reported from the different studies is caused partly by these modelling uncertainties.

(c) It was inferred from limited published information on measured κ values that the quality factor representing upper-crust transmission (Q_{uc}) was on average about 0.2 times the quality factor representing whole-path transmission (Q_o).

(d) An empirical correlation of the whole-path attenuation parameter Q (or Q_o) with the rock shear wave velocity was first developed by collating published information. This correlation was extended to the modelling of κ using Eq. (3) and assuming that Q_{uc}/Q_o is equal to 0.2.

(e) Reference was made to relationships that have been developed to define the magnitude-dependence of κ. The reported relationships were found to have been based on the assumption of near-source activity in high seismic regions, which does not represent the average conditions in regions of low and moderate seismicity.

(f) For seismicity conditions of Australia (as for other intraplate regions), ground shaking intensity was found to have only a minor effect on the value of κ. Thus, applying adjustments to the value of κ for the effects of magnitude, or intensity, does not appear justified.

(g) In parallel with the empirical correlations, values of κ have also been obtained from calibration analyses that employed stochastic simulations of the seismological model (using program GENQKE) along with one-dimensional non-linear shear wave analysis of the rock layers (using program SHAKE). These calibrated κ values have been obtained for soft, average and hard rock layers using the GENQKE-SHAKE analysis procedure.

(h) Values of the κ parameter obtained from the calibration analyses have been superimposed onto the empirical relationships developed earlier in the paper, for comparison purposes. Good agreement between the different approaches has been demonstrated. The κ- shear wave velocity relationship recommended in this paper has thereby been reaffirmed.

Acknowledgements

This paper forms part of the outcome of major strategic research programmes undertaken by the Earthquake Engineering Research Centre at the University of Hong Kong in collaboration with the University of Melbourne to address seismic risk in regions of low and moderate seismicity worldwide. The work described in this paper was substantially supported by a grant from the Research Grants Council of the Hong Kong Special Administrative Region, China (Project No. HKU 7004/02E), whose support is gratefully acknowledged. The Australian programme has been undertaken at the University of Melbourne since 1993, and has received continuous funding from the Australian Commonwealth government. Contributions by Trevor Allen from Geoscience Australia, Canberra through recent discussions are specifically acknowledged. The authors are also very grateful to the invaluable advice given by internationally renowned experts on this subject including Prof. G.F. Panza from Italy; Euan Smith, David Dowrick and Peter Davenport from New Zealand; Prof. Michael Asten at Monash University and Gary Gibson at the Seismology Research Centre, Melbourne. Support over the years by A/Prof. John Wilson and Prof. Graham Hutchinson at the University of Melbourne are also acknowledged.

References

1. Chandler, A.M. and Lam, N.T.K. (2002). "Intensity Attenuation Relationship for the South China Region and Comparison with the Component Attenuation Model", *Journal of Asian Earth Sciences*, **20**(7), 775-790.

2. Lam, N.T.K., Sinadinovski, C., Koo, R.C.H., and Wilson, J.L. (2003). "Peak Ground Velocity Modelling for Australian Earthquakes", *International Journal of Seismology and Earthquake Engineering*, **5**(2), 11-22.

3. Mak, S., Chan, L.S., Chandler, A.M., and Koo, R.C.H. (2004). "Coda Q Estimates in the Hong Kong Region", *Journal of Asian Earth Sciences*, **24**(1), 127-136.

4. Chen, P. and Nuttli, O.W. (1984). "Estimates of Magnitudes and Short-period Wave Attenuation of Chinese Earthquakes from Modified Mercalli Intensity Data", Bulletin of the Seismological Society of America, **74**(3), 957-968.

5. Lam, N.T.K., Wilson, J.L., and Hutchinson, G. (2000). "Generation of Synthetic Earthquake Accelerograms using Seismological Modelling: A Review", *Journal of Earthquake Engineering*, **4**(3), 321-354.

6. Chandler, A.M. and Lam, N.T.K. (2004). "An Attenuation Model for Distant Earthquakes", *Earthquake Engineering and Structural Dynamics*, **33**(2), 183-210.

7. Schnabel, P.B., Lysmer, J., and Seed, H.B. (1972). "A Computer Program for Earthquake Response Analysis of Horizontally Layered sites", Earthquake Engineering Research Centre Report: EERC 72-12, University of California at Berkeley, U.S.A.

8. Abercrombie, R.E. (1997). "Near-Surface Attenuation and Site Effects from Comparison of Surface and Deep Borehole Recordings", Bulletin of the Seismological Society of America, **87**(3), 731-744.

9. Anderson, J.G. and Hough, S.E. (1984). "A Model for the Shape of the Fourier Amplitude Spectrum of Acceleration at High Frequencies", Bulletin of the Seismological Society of America, **74**(5), 1969-1993.

10. Rovelli, A., Bonamassa, O., Cocco, M., Di Bona, M., and Mazza, S. (1988). "Scaling Laws and Spectral Parameters of the Ground Motion in Active Extensional Areas in Italy", Bulletin of the Seismological Society of America, **78**(2), 530-560.

11. Atkinson, G.M. (1996). "The High-Frequency Shape of the Source Spectrum for Earthquakes in Eastern and Western Canada", Bulletin of the Seismological Society of America, **86**(1A), 106-112.

12. Boore, D.M. and Joyner, W.B. (1997). "Site Amplification for Generic Rock Sites", Bulletin of the Seismological Society of America, **87**(2), 327-341.

13. Malagnini, L., Akinci, A., Herrmann, R.B., Alessandro Pino, N. and Scognamiglio, L. (2002). "Characteristics of the Ground Motion in North Eastern Italy", Bulletin of the Seismological Society of America, **92**(6), 2186-2204.

14. Malagnini, L. and Herrmann, R.B. (2000). "Ground-Motion Scaling in the Region of the 1997 Umbria-Marche Earthquake (Italy)", Bulletin of the Seismological Society of America, **90**(4), 1041-1051.

15. Malagnini, L., Herrmann, R.B., and Di Bona, M. (2000). "Ground-Motion Scaling in the Apennines (Italy)", Bulletin of the Seismological Society of America, **90**(4), 1062-1081.

16. Malagnini, L., Herrmann, R.B., and Koch, K. (2000). "Regional Ground-Motion Scaling in Central Europe", Bulletin of the Seismological Society of America, **90**(4), 1052-1061.

17. Bay, F., Fäh, D., Malagnini, L., and Giardini, D. (2003). "Spectral Shear-Wave Ground-Motion Scaling in Switzerland", Bulletin of the Seismological Society of America, **93**(1), 414-429.

18. Ortega, R., Herrmann, R.B., and Quintanar, L. (2003). "Earthquake Ground-motion Scaling in Central Mexico Between 0.7 and 7Hz", Bulletin of the Seismological Society of America, **93**(1), 397-413.

19. Beresnev, I.A. and Atkinson, G.M. (2002). "Source Parameters of Earthquakes in Eastern and Western North America Based on Finite-Fault Modeling", Bulletin of the Seismological Society of America, **92**(2), 695-710.

20. Boatwright, J., Choy, G.L., and Seekins, L.C. (2002). "Regional Estimates of Radiated Seismic Energy", Bulletin of the Seismological Society of America, **92**(4), 1241-1255.

21. Chen, S. and Atkinson, G.M. (2002). "Global Comparisons of Earthquake Source Spectra", Bulletin of the Seismological Society of America,

92(3), 885-895.

22. Raoof, M., Herrmann, R.B., and Malagnini, L. (1999). "Attenuation and Excitation of Three-Component Ground Motion in Southern California", Bulletin of the Seismological Society of America, **89**(4), 888-902.

23. Akinci, A., Malagnini, L., Herrmann, R.B., Alessandro Pino, N., Scognamiglio, L., and Eyidogan, H. (2001). "High-Frequency Ground-Motion in the Erzincan Region, Turkey: Inferences from Small Earthqaukes", Bulletin of the Seismological Society of America, **91**(6), 1446-1455.

24. Singh, S.K., Bansal, B.K., Bhattacharya, S.N., Pacheco, J.F., Dattatrayam, R.S., Ordaz, M., Suresh, G., Kamal, and Hough, S.E. (2003). "Estimation of Ground Motion for Bhuj (26 January 2001; Mw 7.6) and for Future Earthquakes in India", Bulletin of the Seismological Society of America, **93**(1), 353-370.

25. Wilkie, J. and Gibson, G. (1995). "Estimation of Seismic Quality Factor Q for Victoria, Australia", *Journal of Australian Geology and Geophysics*, **15**(4), 511-517.

26. Jin, A. and Aki, K. (1988). "Spatial and Temporal Correlation between Coda *Q* and Seismicity in China", Bulletin of the Seismological Society of America, **78**(2), 741-769.

27. Global Crustal Model CRUST2.0 (2001). Institute of Geophysics and Planetary Physics, The University of California, San Diego. Website: http://mahi.ucsd.edu/Gabi/rem.dir/crust/crust2.html.

28. Mooney, W.D., Laske, G., and Masters, T.G. (1998). "CRUST 5.1: A Global Crustal Model at 5º × 5º", *Journal of Geophysical Research*, **103**, 727-747.

29. Chandler, A.M., Lam, N.T.K., and Tsang, H.H. (2005). "Shear Wave Velocity Modelling in Bedrock for Analysis of Intraplate Seismic Hazard", *Soil Dynamics and Earthquake Engineering*, **25**, 167-185.

30. Frankel, A., Mueller, C., Barnhard, T., Perkins, D., Leyendecker, E., Dickman, N., Hanson, S., and Hopper, M. (1996). "National Seismic Hazard Maps, June 1996", U.S. Geol. Surv. Open-File Rept. 96-532.

31. Margaris, B.N. and Hatzidimitriou, P.M. (2002). "Source Spectral Scaling and Stress Release Estimates Using Strong-motion Records in Greece", Bulletin of the Seismological Society of America, **92**(3), 1040-1059.

32. Atkinson, G.M. and Silva, W. (1997). "An Empirical Study of Earthquake Source Spectra for California Earthquakes", Bulletin of the Seismological Society of America, **87**(1), 97-113.

33. Atkinson, G.M. and Boore, D.M. (1998). "Evaluation of Models for Earthquake Source Spectra in Eastern North America", Bulletin of the Seismological Society of America, **88**(4), 917-937.

34. Atkinson, G.M. and Silva, W. (2000). "Stochastic Modeling of California Ground Motions", Bulletin of the Seismological Society of America, **90**(2), 255-274.

35. Housner, G.W. (1959). "Behaviour of Structures during Earthquakes", *Journal of the American Society of Civil Engineers*, 109-129.

36. Lam, N.T.K. (1999). "Program 'GENQKE' User's Guide". Department of Civil and Environmental Engineering, The University of Melbourne, Australia.

37. Melchers, R.E. (ed.) (1990). "Newcastle Earthquake Study". The Institution of Engineers, Australia.

38. AS1170.4 (1993). "Standards Association of Australia. Minimum Design Loads on Structures: Part 4: Earthquake Loads-AS1170.4 and Commentary".

39. Worthington, M.H., King, M.S., and Marsden, J.R. (2001). "Determining the Damping Factor of Sedimentary Rocks Required for Seismically Designed Structures", *International Journal of Rock Mechanics and Mining Science*, **38**(6), 801-806.

40. Lam, N.T.K. and Wilson, J.L. (1999). "Estimation of the Site Natural Period from Borehole

Records", *Australian Journal of Structural Engineering*, **SE1**(3), 179-199.

41. Nishi, K., Ishiguro, T., and Kudo, K. (1989). "Dynamic Properties of Weathered Sedimentary Soft Rock", Soils Foundation Japan, **20**, 67-82.

42. Borden, R.H., Shao, L.S., and Gupta, A. (1996). "Dynamic Properties of Piedmont Residual Soils", *Journal of Geotechnical Engineering*, **122**(10), 813-821.

43. Kim, D.S., Stokoe, K.H., and Roesset, J.M. (1991). "Characterization of Material Damping of Soils Using Resonant Column and Torsional Shear Tests", *Proceedings of the 5th International Conference Soil Dynamic and Earthquake Engineering*, Karlruhe, 189-200.

44. Nishi, K., Kokusho, T., and Esashi, Y. (1983). "Dynamic Shear Modulus and Damping Ratio of Rocks for a Wide Confining Pressure Range", *Proceedings of the Fifth Congress International Society for Rock Mechanics*, Melbourne, **2**, 223-226.